INORGANIC CHEMISTRY FRONTIERS

RESEARCH ARTICLE

Cite this: *Inorg. Chem. Front.*, 2022, **9**, 1016

Organometallic Ni(II), Ni(III), and Ni(IV) complexes relevant to carbon–carbon and carbon–oxygen bond formation reactions†

C. Magallón, [a] L. Griego,[b] C. H. Hu,[b] A. Company, *[a] X. Ribas *[a] and L. M. Mirica *[b]

Received 27th November 2021,
Accepted 13th January 2022

DOI: 10.1039/d1qi01486b

rsc.li/frontiers-inorganic

Herein, the pyridinophanetetradentate ligand 3,6,9-trimethyl-3,6,9,15-tetraazabicyclo[9.3.1]pentadeca-1(15),11,13-triene, $PyNMe_3$, is used to isolate and structurally characterize well-defined organometallic Ni(II) and Ni(III) complexes bearing the cycloneophyl fragment, an alkyl/aryl C-donor ligand. Furthermore, spectroscopic and cryo-mass spectrometry studies suggest the formation of a transient Ni(IV) organometallic complex, and its relevance to C–C and C–O bond formation reactivity studies is discussed.

Introduction

The formation of new C–C and C–heteroatom bonds through transition-metal catalyzed cross-coupling reactions (*i.e.*, Suzuki, Kumada, and Negishi reactions) is currently one of the most powerful tools in organic chemistry.[1–3] In this context, noble metal-based systems are the more commonly used catalysts for these transformations, due to their widely understood mechanism.[4–7] For example, Pd-catalyzed reactions usually occur *via* Pd^0/Pd^{II} catalytic cycles and mostly involve diamagnetic intermediate species, which makes their characterization more feasible.[8] In contrast, the mechanisms of Ni-catalyzed cross-coupling reactions are far less understood since this first-row transition metal can easily undergo both one- and two-electron redox processes, often involving paramagnetic intermediate species that lead to more complex mechanistic pathways.[9–11] Although traditionally Ni-catalyzed cross-coupling reactions have been reported to involve Ni^0, Ni^I and Ni^{II} intermediates,[12–14] recent studies suggest that high-valent Ni^{III} and Ni^{IV} species are key intermediates in the C–C/C–heteroatom bond-forming step.[15–24]

Pyridinophanetetradentate ligands have been shown to stabilize uncommon high-valent organometallic nickel complexes. Indeed, in the past several years, Mirica and co-workers have employed a series of tetradentatepyridinophane ligands with different amine N-substituents ($^RN4$ ligands, R = Me, Ts, ^{i}Pr, ^{t}Bu, and Np) as well as the tridentate 1,4,7-trimethyl-1,4,7-triazacyclononane ligand (Me_3tacn) to stabilize $Ni^{III/IV}$ complexes (Fig. 1a), as well as $Pd^{II/IV}$ complexes, that undergo

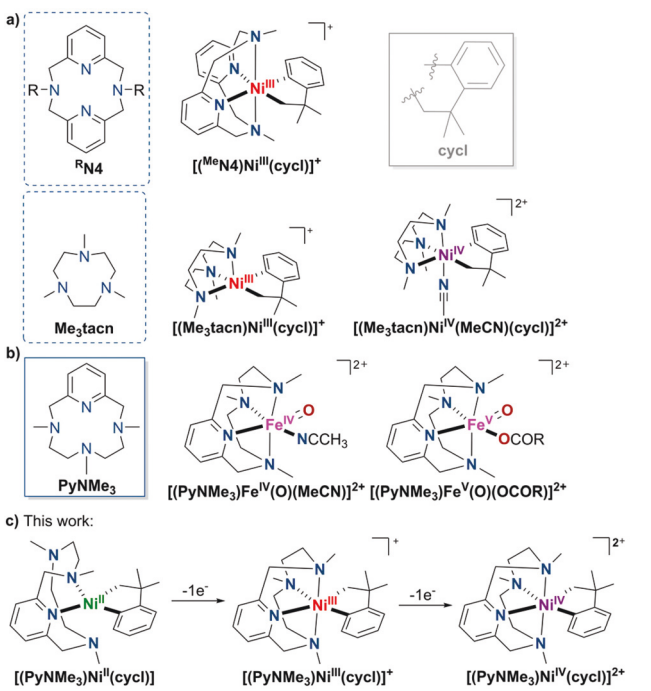

Fig. 1 (a) Isolated organometallic nickel complexes bearing tridentate or tetradentate N-donor ligands and cycloneophyl as the C-donor ligand; (b) spectroscopically characterized high-valent iron-oxo intermediate species relevant for O_2 activation chemistry bearing the tetradentate N-based $PyNMe_3$ ligand, and (c) synthesis of well-defined organometallic nickel complexes bearing the $PyNMe_3$ and cycloneophyl ligands and their C–C and C–O bond formation reactivity.

[a]*Institut de QuímicaComputacional i Catàlisi (IQCC) and Departament de Química, Universitat de Girona, Campus Montilivi, Girona, E-17003 Catalonia, Spain. E-mail: anna.company@udg.edu, xavi.ribas@udg.edu*

[b]*Department of Chemistry, University of Illinois at Urbana-Champaign, 600 S. Mathews Avenue, Urbana, Illinois 61801, USA. E-mail: mirica@illinois.edu*

†Electronic supplementary information (ESI) available: Additional information. CCDC 2118410 (**1-Br**), 2118413 (**1-Cl**), 2118411 (**2**) and 2118412 (**3**). For ESI and crystallographic data in CIF or other electronic format see DOI: 10.1039/d1qi01486b

C–C/C–heteroatom bond formation reactions.[25–40] Recently, a macrocyclic N-based tetradentate ligand $PyNMe_3$ has been employed by Costas, Company and co-workers to stabilize high-valent intermediate species and has proved to be successful to trap $Fe^{IV/V}$-oxo species (Fig. 1b) and dinuclear Cu^{II} side-on peroxo species.[41–45] However, the use of the $PyNMe_3$ ligand has never been employed to explore the reactivity of organometallic Ni complexes.

Herein we report the synthesis, characterization, and initial reactivity studies of a series of organometallic Ni^{II}, Ni^{III} and Ni^{IV} complexes supported by the $PyNMe_3$ ligand and containing the cycloneophyl fragment, an alkyl/aryl C-donor ligand (Fig. 1c). The cycloneophyl ligand was developed by Carmona *et al.* as an ancillary ligand to isolate organonickel complexes, since the resulting Ni(cycloneophyl) complexes are less prone to reductive elimination or β-hydride elimination.[46–48] In addition, the cycloneophyl moiety has been widely and successfully employed together with N-based ligands independently by Sanford and Mirica in order to study C–C and C–heteroatom bond forming reactions.[31–33,49–54] The current study reports the reactivity of the isolated $[(PyNMe_3)Ni^{II}(cycl)]$ complex with oxidants to promote C–C or C–O reductive elimination through Ni^{IV} intermediate species.

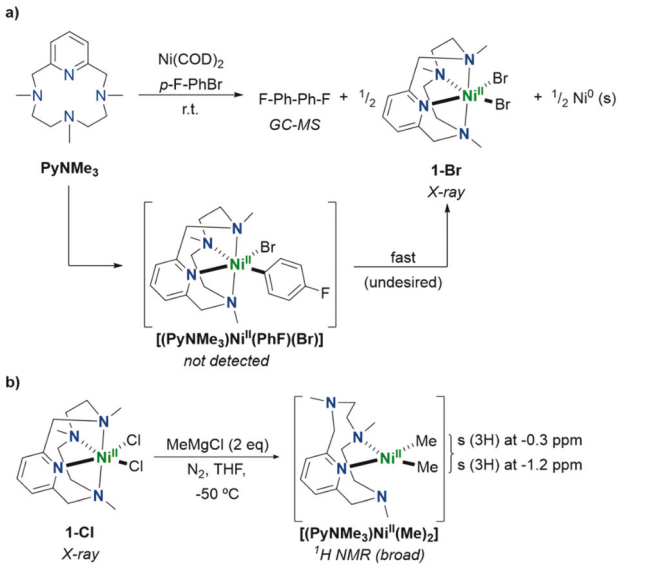

Fig. 2 (a) Attempt to synthesize **[(PyNMe$_3$)Ni^{II}(PhF)(Br)]** *via* oxidative addition at nickel(0), and (b) attempt to synthesize **[(PyNMe$_3$)Ni^{II}(Me)$_2$]** *via* transmetallation at the nickel(II)–chloride precursor, **1-Cl**.

Results and discussion

Our first attempt to isolate organometallic nickel complexes bearing the $PyNMe_3$ ligand consisted of the *in situ* oxidative addition of 1-bromo-4-fluorobenzene using $Ni(cod)_2$. The putative $[(PyNMe_3)Ni^{II}(pF\text{-}Ph)(Br)]$ complex could not be isolated due to fast decomposition and rapid ligand exchange that leads to the formation of 0.5 equiv. of $[(PyNMe_3)Ni^{II}Br_2]$ (**1-Br**) and 0.5 equiv. of $[(PyNMe_3)Ni^{II}(pF\text{-}Ph)_2]$. The latter di-aryl complex then undergoes reductive elimination to afford the homocoupled product *p*F-Ph-Ph-*p*F (as detected *via* GC-MS), free ligand and Ni(0) (Fig. 2a). In addition, the reaction of $[(PyNMe_3)Ni^{II}(Cl)_2]$ (**1-Cl**) with MeMgCl in THF at −50 °C led to an intractable mixture due to the fast decomposition of the desired nickel(II)–dimethyl complex (Fig. 2b). Nonetheless, the putative $[(PyNMe_3)Ni^{II}(Me)_2]$ species could be detected *via* ^{1}H NMR, which revealed two singlets below 0 ppm that integrated to three protons each and presumably corresponded to the two inequivalent methyl groups directly attached to the Ni center (Fig. S1†).

Gratifyingly, the combination of $PyNMe_3$ and cycloneophyl ($-CH_2CMe_2\text{-}o\text{-}C_6H_4-$, or cycl) as ligands allows the stabilization and isolation of complex $[(PyNMe_3)Ni^{II}(cycl)]$ (**2**) in 67% yield. The complex was synthesized *via* ligand exchange of the Ni(II) precursor $[(py)_2Ni^{II}(cycl)]$ with an equimolar amount of $PyNMe_3$ in 1 : 1 toluene/pentane, for 16 hours at room temperature under a nitrogen atmosphere (Fig. 3a). The X-ray structure revealed a square planar geometry around the Ni(II) center, with the $PyNMe_3$ ligand coordinated in a bidentate fashion (Fig. 3b). This new system allows for the observation of the *trans* influence of the ligands. Interestingly, the $PyNMe_3$

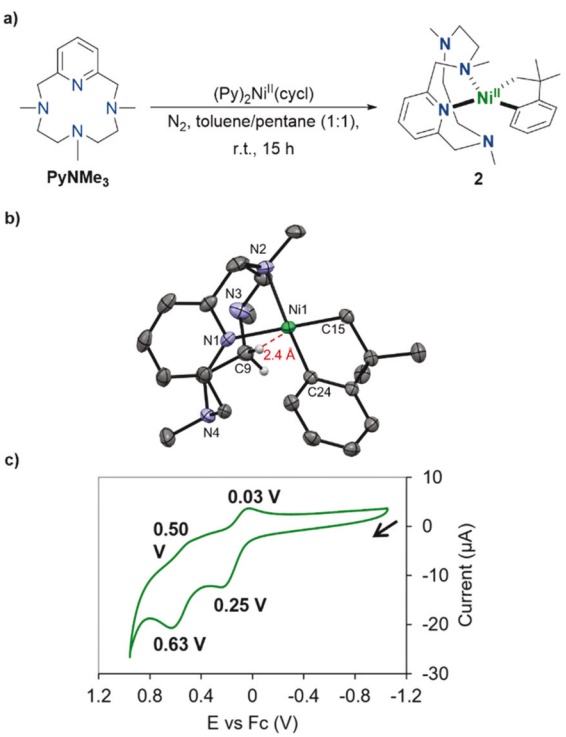

Fig. 3 (a) Synthesis and characterization of complex **[(PyNMe$_3$)Ni^{II}(cycl)]**, **2**; (b) ORTEP representation of **2** (50% probability thermal ellipsoids; hydrogen atoms have been omitted for clarity; selected distances (Å): Ni–C24, 1.888(2); Ni–C15, 1.932(2); Ni–N2, 2.0535(19); Ni–N1, 1.9923(19), and c) CV of **2** in 0.1 M $NBu_4(PF_6)$/MeCN at a scan rate of 100 mVs^{-1} (Ag wire as a reference electrode).

ligand coordinates to the Ni(II) center through the pyridine moiety which is *trans* to the alkyl ligand, and one of the adjacent amines *trans* to the phenyl group. This type of coordination could not be observed with the previously reported systems bearing symmetric pyridinophane type ligands (^{R}N4). In addition, the ^{1}H-NMR spectrum confirms that **2** is a low-spin diamagnetic Ni(II) complex. Detailed NMR experiments were used to assign all proton and carbon peaks for **2** (Fig. S2–S9†).The broadness of the peaks, especially the methylene protons on the PyNMe$_3$ ligand, is likely due to the rapid ligand exchange of the four types of N donors. Furthermore, the unusual Ni(II) structure allows for an anagostic interaction of the methylene protons vicinal to the tertiary amine and the Ni metal center, with a Ni···H distance of 2.40 Å and a Ni···H–C9 angle of 170°. The cyclic voltammogram (CV) of **2** in 0.1 M (nBu$_4$N)PF$_6$/MeCN reveals a quasi-reversible redox event at $E_{1/2}$ = 250 mV *vs.* ferrocene (Fc), followed by another quasi-reversible oxidation at $E_{1/2}$ = 630 mV (Fig. 3c). These observed pseudo-reversible oxidations are presumably assigned to the $Ni^{III/II}$ and $Ni^{IV/III}$ redox couples, respectively. This result suggests accessible Ni(III) and Ni(IV) species, likely due to the stabilizing effect of the two anionic chelating C donors from the cycloneophyl ligand, as well as the tetradentate PyNMe$_3$ ligand, as reported previously for high-valent iron-oxo species.[27,33,37]

In fact, **2** was rapidly oxidized with 1 equiv. of ferrocenium hexafluorophosphate (FcPF$_6$) in MeCN at −35 °C to yield the reddish product [(PyNMe$_3$)Ni^{III}(cycl)](PF$_6$), **3** (Fig. 4a). The EPR spectrum of **3** in 1 : 3 MeCN/PrCN is consistent with a Ni(III) d^7 complex and exhibits a pseudoaxial signal with superhyperfine coupling to two nitrogen atoms in the g_z direction (A_{2N} = 13.7 G), indicating that two I = 1 nitrogen atoms, presumably from the ligand and/or solvent, coordinate to the Ni(III) center (Fig. 4b). Luckily, complex **3** was stable and isolated at low temperature in 73% yield.

The single crystal X-ray structure of **3** confirmed the six-coordinate Ni(III) center in a distorted octahedral geometry where the 6 coordination positions are occupied by the PyNMe$_3$ and cycloneophyl ligands, thus confirming the EPR data (Fig. 4c). Intriguingly, both the Ni–N and Ni–C distances in **3** are longer than those in **2**, as previously observed for similar complexes, and are likely due to the change in the coordination number from 4 to 6 upon oxidation.[33,37] Moreover, cryo-ESI-mass spectrometry at −40 °C was performed to further characterize this Ni(III) complex. The MS spectrum showed a major monocharged peak with m/z = 438.2289 and an isotopic pattern fully consistent with the calculated values for $\mathbf{3}^{+}$, $[(C_{14}H_{24}N_4)Ni^{III}(C_{10}H_{12})]^{+}$ (Fig. 4d).

Attempts to synthesize the corresponding Ni(IV) complex were conducted through a stepwise oxidation of **2**. The oxidation of **2** to obtain **3** was monitored by low-temperature UV/vis spectroscopy (Fig. 5a and b). This experiment was performed at−40 °C using a 0.5 mM solution of **2** in MeCN. An initial spectrum was recorded for the starting Ni(II) complex, which exhibited an absorption band with λ_{max} = 462 nm. For the one-electron oxidation of each complex monitored by low-temperature UV/vis, NO(SbF$_6$) was used as an oxidant in order to obtain a cleaner spectrum, since Fc^{+} exhibits two absorption bands at 325 nm and 440 nm that could interfere with the detection of new species. Thus, the addition of 1 equiv.of NO^{+} to **2** immediately yields **3**, which exhibits an absorption band with λ_{max} = 513 nm. Afterwards, another equivalent of the same oxidant was added to generate the new Ni(IV) complex, **4**. Upon addition of the second equivalent of the oxidant, the UV/

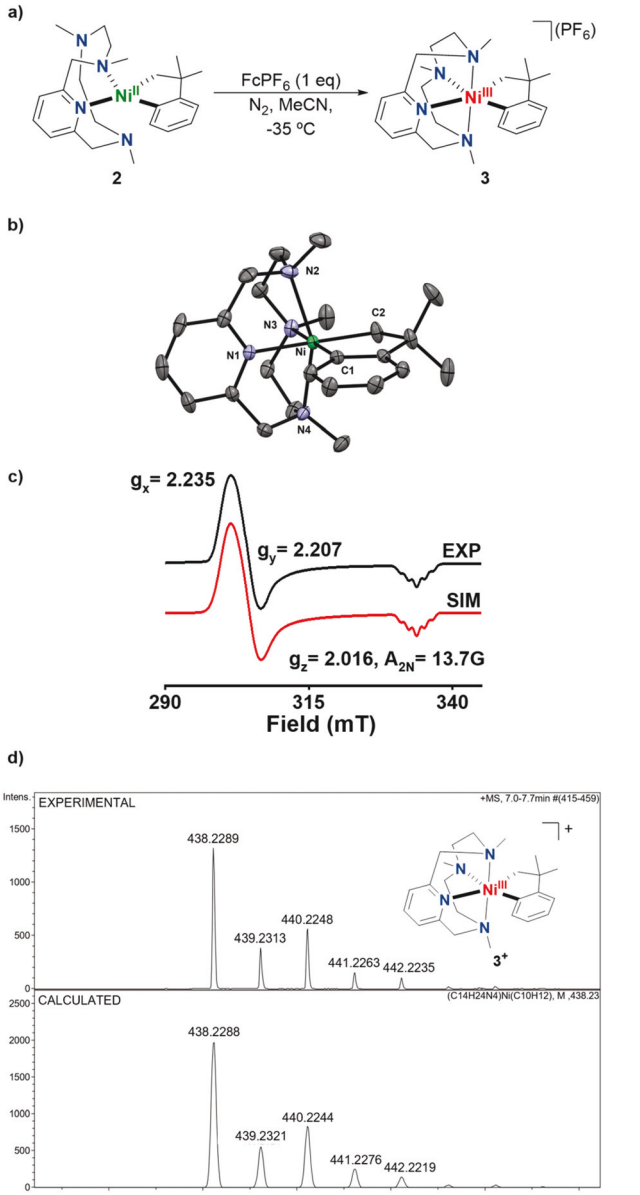

Fig. 4 (a) Synthesis and characterization of complex **[(PyNMe$_3$)Ni^{III}(cycl)](PF$_6$)**, **3**; (b) ORTEP representation of **3** (50% probability thermal ellipsoids; hydrogen atoms have been omitted for clarity; selected distances (Å): Ni–C1, 1.9492 (12); Ni–C2, 1.9693 (14); Ni–N1, 1.9944 (11); Ni–N2, 2.2543 (13); Ni–N3, 2.1463 (12); Ni–N4, 2.2470 (12); (c) EPR spectra of complex 3 at 77 K in 1 : 3 MeCN/PrCN (black: experimental; red: simulated); and (d) cryo-HR-MS of **3** showing the monocationic peak ($\mathbf{3}^{+}$) at m/z = 438.2289 (top) and the simulation of its isotopic pattern (bottom).

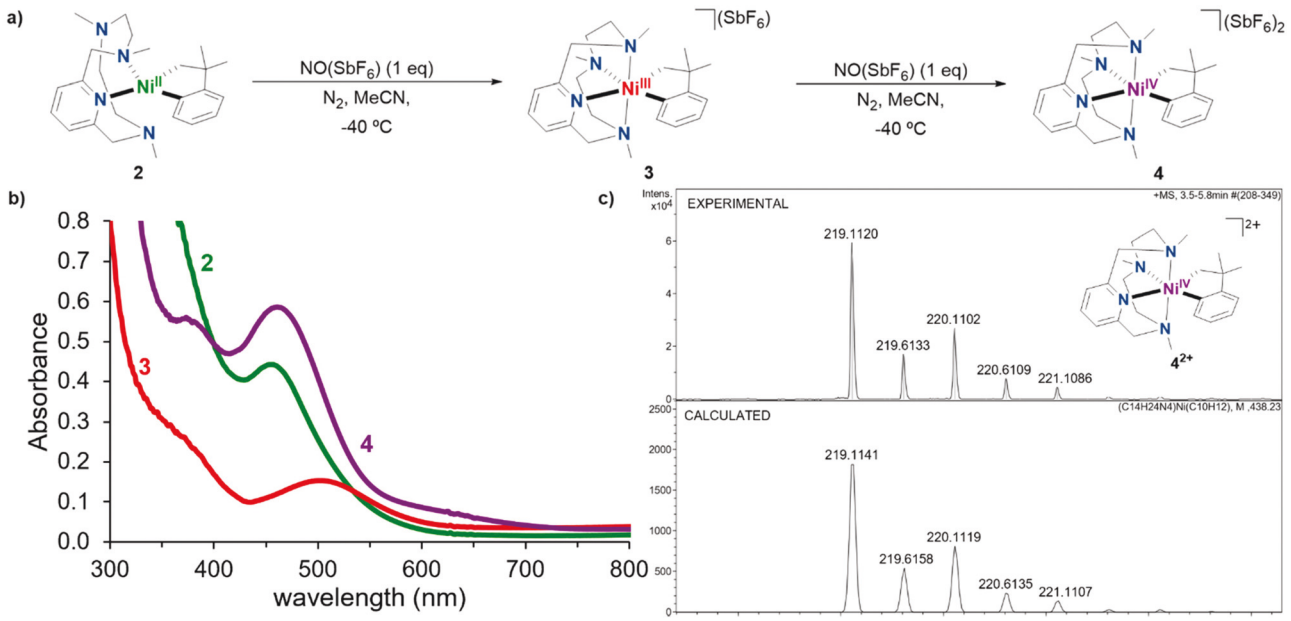

Fig. 5 (a) Step-wise one-electron oxidation to nickel(IV) from **2** using $NO(SbF_6)$ as an oxidant; (b) UV-vis characterization of complexes **2**, **3** and **4** obtained by the consecutive one-electron oxidation of **2** with $NO(SbF_6)$, respectively, and (c) cryo-HR-MS of **4** showing the dicationic peak ($\mathbf{4}^{2+}$) at m/z = 219.1120 (top) and simulation of its isotopic pattern (bottom).

vis spectrum instantly changed and showed the formation of two absorption bands with a λ_{max} of 384 nm and 470 nm, and a shoulder at 620 nm (Fig. 5b). The subsequent injection of an aliquot into the cryo-ESI-mass spectrometer confirmed the generation of species **4** with a dicationic major peak with a mass value of m/z = 219.1120 and an isotopic pattern fully consistent with the calculated value for $[(C_{14}H_{24}N_4)Ni^{IV}(C_{10}H_{12})]^{2+}$ (Fig. 5c). This novel complex was further characterized by NMR spectroscopy, where a stepwise injection of 2 equiv. of NO^+ resulted in the observation of a new Ni(IV) species (Fig. S10 and S11†).

In line with the UV-vis results, monitoring the oxidation by NMR provided complementary information. A color change from orange to red-pink was observed upon the addition of 1 equiv. of oxidant in CD_3CN at −35 °C, while the obtained paramagnetic NMR spectrum supported the formation of a Ni(III) species. Interestingly, a second equivalent of oxidant allowed the formation of a new diamagnetic species, tentatively assigned as a Ni(IV) complex. The inherent broadness of the NMR spectrum of the putative Ni(IV) species was likely caused by the residual Ni(III), which made peak assignment difficult. However, the obtained Ni(IV) spectrum closely resembles those of the recently reported Ni^{IV}–cycloneophyl complexes supported by the N-based ligands pyridinophane (^{Me}N4) and triazacyclononane (^{Me}tacn).[32,37] Due to the highly electrophilic nature of the Ni(IV) species, a key structural feature observed in both ^{Me}N4 and ^{Me}tacnNi^{IV}–cyclonephyl systems was a large shift of the Ni^{IV}–CH_2– protons from ~2.10 ppm in their Ni^{II}–CH_2–counterparts to 5.33 ppm and 5.50 ppm, respectively. A similar shift was observed with **4**, in which the Ni^{IV}–CH_2–protons shifted to 5.29 ppm, similar to what was observed for (^{Me}tacn)Ni^{IV}(cycl).[32]

Next, we focused on the reactivity of **3** and **4** in C–C or C–O bond formation reactions. First, we exposed the Ni^{III} species **3** to high temperatures (80 °C) to evaluate its stability, and it was found that the compound decomposed to an intractable mixture, which contained ~15% of the protodemetalation product *t*-butylbenzene, and yet no reductive elimination products were obtained. Then, since the Ni(IV) complex **4** was metastable, we studied its reactivity by generating it *in situ* through the oxidation of **2** with a variety of two-electron oxidants such as XeF_2, 1-fluoro-2,4,6-trimethylpyridinium triflate (NFTPT), and $PhI(OAc)_2$, and yet no appreciable amount of any reductive elimination products were observed. In contrast, promising results were obtained when exploring its reactivity with green oxidants such as O_2, H_2O_2, and ^{t}BuOOH (Fig. 6).

In these reactions, only a trace amount (<1%) of the protodemetalation product *t*-butylbenzene, **B**, was observed in GC-MS, indicating a nearly full conversion of **2** into the corresponding Ni^{III}/Ni^{IV} species. The reaction of **2** with 2 equiv. of

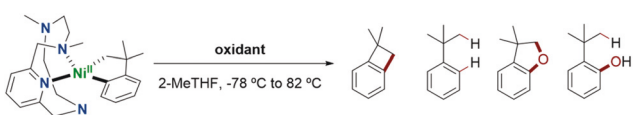

Entry	Oxidant	A	B	C	D
1	O_2	59 %	0 %	6 %	2 %
2	H_2O_2	9 %	1 %	11 %	2 %
3	$^tBuO_2H$	3 %	1 %	8 %	3 %

GC-MS

Fig. 6 Reactivity studies of **2** with different two-electron oxidants, and the quantification of the respective organic products by GC-MS.

H_2O_2 in 2-MeTHF results in the formation of 11% **C** and 9% **A** as the primary organic products. The reaction of **2** with ^{t}BuOOH shows a similar distribution of products. On the other hand, the reaction of **2** with dioxygen generated up to 59% of C–C coupled product **A**, exhibiting an appreciable C–C bond formation reactivity, which is proposed to occur *via* the intermediacy of the Ni(IV) species **4**. It is important to note that this tetradentate $PyNMe_3$ ligand system displays a different reactivity from the structurally related pyridinophane ^{R}N4 system,[33] where C–O reductive elimination was greatly enhanced. In this case, it is likely that a Ni^{IV}–hydroxo transient, yet metastable intermediate was generated and led to competing C–C/C–O reductive elimination steps, which has been observed for M^{IV}complexes (M = Pt, Pd) bearing ligands that are prone to reductive elimination.[32,33]By contrast, the [($PyNMe_3$)Ni(cycl)] system seems to favor the C–C bond formation reactivity over the formation of any oxygen-containing products, possibly because the $PyNMe_3$ ligand is flexible enough to strongly bind to the Ni(IV) species and complete the octahedral coordination geometry, without allowing the coordination of any additional oxidant-derived, O-donor ligand.

Conclusion

In summary, we have been able to explore the rich organometallic redox chemistry of Ni by characterizing spectroscopically Ni^{II} (**2**), Ni^{III} (**3**) and Ni^{IV} (**4**) complexes supported by the tetradentate N-donor ligand $PyNMe_3$. **2** features a square-planar geometry with two pendant aliphatic amine moieties, which enter into the coordination sphere of the metal upon oxidation to a Ni(III), **3**, that features a distorted octahedral geometry. Further reaction of **3** with another equivalent of oxidant affords the putative Ni(IV) complex **4**. Reactivity studies indicated that the *in situ* formed Ni(IV) complex, [($PyNMe_3$)Ni^{IV}(cycl)][SbF_6)$_2$ (**4**), promotes C–C coupling over C–O coupling despite the use of O-based oxidants, in contrast to the related pyridinophane ^{R}N4 systems.[33] Overall, this new $PyNMe_3$ ligand system provides important insight for understanding at the molecular level the electronic properties of dissymmetric macrocyclic ligands on well-defined Ni^{II} (**2**), Ni^{III} (**3**) and Ni^{IV} (**4**) organometallic complexes and their role in C–C and C–O bond formation transformations.

Conflicts of interest

There are no conflicts to declare.

Acknowledgements

We acknowledge financial support from NSF CHE-1925751 to L.M., MINECO-Spain for projects PID2019-104498GB-I00 to X.R., and PID2019-106699GB-I00 to A.C. Generalitat de Catalunya is also acknowledged for project 2017SGR264. We thank UdG for a IFUdG PhD grant to C.M. X.R. and A.C. are thankful for an ICREA Acadèmia award. The authors are grateful to STR-UdG for technical support.

Notes and references

1 F. Diederich and A. de Meijere, *Metal-Catalyzed Cross-Coupling Reactions*, Wiley-VCH, Weinheim, Germany, 2nd edn, 2004.
2 J. F. Hartwig, *Organotransition Metal Chemistry: From Bonding to Catalysis*, University Science Books, Sausalito, 2010.
3 J. Terao and N. Kambe, Cross-Coupling Reaction of Alkyl Halides with Grignard Reagents Catalyzed by Ni, Pd, or Cu Complexes with π-Carbon Ligand(s), *Acc. Chem. Res.*, 2008, **41**, 1545–1554.
4 J. Magano and J. R. Dunetz, Large-Scale Applications of Transition Metal-Catalyzed Couplings for the Synthesis of Pharmaceuticals, *Chem. Rev.*, 2011, **111**, 2177–2250.
5 J.-P. Corbet and G. Mignani, Selected Patented Cross-Coupling Reaction Technologies, *Chem. Rev.*, 2006, **106**, 2651–2710.
6 C. C. C. Johansson Seechurn, M. O. Kitching, T. J. Colacot and V. Snieckus, Palladium-Catalyzed Cross-Coupling: A Historical Contextual Perspective to the 2010 Nobel Prize, *Angew. Chem., Int. Ed.*, 2012, **51**, 5062–5085.
7 J. F. Hartwig, Carbon–Heteroatom Bond-Forming Reductive Eliminations of Amines, Ethers, and Sulfides, *Acc. Chem. Res.*, 1998, **31**, 852–860.
8 J. F. Hartwig, Carbon–heteroatom bond formation catalysed by organometallic complexes, *Nature*, 2008, **455**, 314–322.
9 X. Hu, Nickel-catalyzed cross coupling of non-activated alkyl halides: a mechanistic perspective, *Chem. Sci.*, 2011, **2**, 1867–1886.
10 V. B. Phapale and D. J. Cárdenas, Nickel-catalysed Negishi cross-coupling reactions: scope and mechanisms, *Chem. Soc. Rev.*, 2009, **38**, 1598–1607.
11 T. T. Tsou and J. K. Kochi, Reductive coupling of organometals induced by oxidation. Detection of metastable paramagnetic intermediates, *J. Am. Chem. Soc.*, 1978, **100**, 1634–1635.
12 T. T. Tsou and J. K. Kochi, Mechanism of oxidative addition. Reaction of nickel(0) complexes with aromatic halides, *J. Am. Chem. Soc.*, 1979, **101**, 6319–6332.
13 J. Cornella, E. Gómez-Bengoa and R. Martin, Combined Experimental and Theoretical Study on the Reductive Cleavage of Inert C–O Bonds with Silanes: Ruling out a Classical Ni(0)/Ni(II) Catalytic Couple and Evidence for Ni(I) Intermediates, *J. Am. Chem. Soc.*, 2013, **135**, 1997–2009.
14 C. A. Laskowski, D. J. Bungum, S. M. Baldwin, S. A. Del Ciello, V. M. Iluc and G. L. Hillhouse, Synthesis and Reactivity of Two-Coordinate Ni(I) Alkyl and Aryl Complexes, *J. Am. Chem. Soc.*, 2013, **135**, 18272–18275.
15 L. M. Mirica, S. M. Smith and L. Griego, Organometallic Chemistry of High-Valent Ni(III) and Ni(IV) Complexes, in

Nickel Catalysis in Organic Synthesis, ed. S. Ogoshi, 2020, pp. 223–248.

16 A. Joshi-Pangu, C.-Y. Wang and M. R. Biscoe, Nickel-Catalyzed Kumada Cross-Coupling Reactions of Tertiary Alkylmagnesium Halides and Aryl Bromides/Triflates, *J. Am. Chem. Soc.*, 2011, **133**, 8478–8481.

17 A. S. Dudnik and G. C. Fu, Nickel-Catalyzed Coupling Reactions of Alkyl Electrophiles, Including Unactivated Tertiary Halides, To Generate Carbon–Boron Bonds, *J. Am. Chem. Soc.*, 2012, **134**, 10693–10697.

18 N. D. Schley and G. C. Fu, Nickel-Catalyzed Negishi Arylations of Propargylic Bromides: A Mechanistic Investigation, *J. Am. Chem. Soc.*, 2014, **136**, 16588–16593.

19 J. C. Tellis, D. N. Primer and G. A. Molander, Single-electron transmetalation in organoboron cross-coupling by photoredox/nickel dual catalysis, *Science*, 2014, **345**, 433–436.

20 Z. Zuo, D. T. Ahneman, L. Chu, J. A. Terrett, A. G. Doyle and D. W. C. MacMillan, Merging photoredox with nickel catalysis: Coupling of α-carboxyl sp3-carbons with aryl halides, *Science*, 2014, **345**, 437–440.

21 J. Cornella, J. T. Edwards, T. Qin, S. Kawamura, J. Wang, C.-M. Pan, R. Gianatassio, M. Schmidt, M. D. Eastgate and P. S. Baran, Practical Ni-Catalyzed Aryl–Alkyl Cross-Coupling of Secondary Redox-Active Esters, *J. Am. Chem. Soc.*, 2016, **138**, 2174–2177.

22 S. Z. Tasker, E. A. Standley and T. F. Jamison, Recent advances in homogeneous nickel catalysis, *Nature*, 2014, **509**, 299–309.

23 J. R. Bour, N. M. Camasso, E. A. Meucci, J. W. Kampf, A. J. Canty and M. S. Sanford, Carbon–Carbon Bond-Forming Reductive Elimination from Isolated Nickel(III) Complexes, *J. Am. Chem. Soc.*, 2016, **138**, 16105–16111.

24 N. M. Camasso and M. S. Sanford, Design, synthesis, and carbon-heteroatom coupling reactions of organometallic nickel(IV) complexes, *Science*, 2015, **347**, 1218–1220.

25 J. R. Khusnutdinova, N. P. Rath and L. M. Mirica, Stable Mononuclear Organometallic Pd(III) Complexes and Their C–C Bond Formation Reactivity, *J. Am. Chem. Soc.*, 2010, **132**, 7303–7305.

26 J. R. Khusnutdinova, N. P. Rath and L. M. Mirica, Dinuclear Palladium(III) Complexes with a Single Unsupported Bridging Halide Ligand: Reversible Formation from Mononuclear Palladium(II) or Palladium (IV) Precursors, *Angew. Chem., Int. Ed.*, 2011, **50**, 5532–5536.

27 J. R. Khusnutdinova, N. P. Rath and L. M. Mirica, The Aerobic Oxidation of a Pd(II) Dimethyl Complex Leads to Selective Ethane Elimination from a Pd(III) Intermediate, *J. Am. Chem. Soc.*, 2012, **134**, 2414–2422.

28 F. Tang, Y. Zhang, N. P. Rath and L. M. Mirica, Detection of Pd(III) and Pd(IV) Intermediates during the Aerobic Oxidative C–C Bond Formation from a Pd(II) Dimethyl Complex, *Organometallics*, 2012, **31**, 6690–6696.

29 F. Tang, F. Qu, J. R. Khusnutdinova, N. P. Rath and L. M. Mirica, Structural and reactivity comparison of analogous organometallic Pd(III) and Pd(IV) complexes, *Dalton Trans.*, 2012, **41**, 14046–14050.

30 J. R. Khusnutdinova, N. P. Rath and L. M. Mirica, The Conformational Flexibility of the Tetradentate Ligand tBuN4 is Essential for the Stabilization of (tBuN4)PdIII Complexes, *Inorg. Chem.*, 2014, **53**, 13112–13129.

31 F. Qu, J. R. Khusnutdinova, N. P. Rath and L. M. Mirica, Dioxygen activation by an organometallic Pd(ii) precursor: formation of a Pd(iv)–OH complex and its C–O bond formation reactivity, *Chem. Commun.*, 2014, **50**, 3036–3039.

32 M. B. Watson, N. P. Rath and L. M. Mirica, Oxidative C–C Bond Formation Reactivity of Organometallic Ni(II), Ni(III), and Ni(IV) Complexes, *J. Am. Chem. Soc.*, 2017, **139**, 35–38.

33 S. M. Smith, O. Planas, L. Gómez, N. P. Rath, X. Ribas and L. M. Mirica, Aerobic C–C and C–O bond formation reactions mediated by high-valent nickel species, *Chem. Sci.*, 2019, **10**, 10366–10372.

34 B. Zheng, F. Tang, J. Luo, J. W. Schultz, N. P. Rath and L. M. Mirica, Organometallic Nickel(III) Complexes Relevant to Cross-Coupling and Carbon–Heteroatom Bond Formation Reactions, *J. Am. Chem. Soc.*, 2014, **136**, 6499–6504.

35 F. Tang, N. P. Rath and L. M. Mirica, Stable bis(trifluoromethyl)nickel(III) complexes, *Chem. Commun.*, 2015, **51**, 3113–3116.

36 W. Zhou, J. W. Schultz, N. P. Rath and L. M. Mirica, Aromatic Methoxylation and Hydroxylation by Organometallic High-Valent Nickel Complexes, *J. Am. Chem. Soc.*, 2015, **137**, 7604–7607.

37 J. W. Schultz, K. Fuchigami, B. Zheng, N. P. Rath and L. M. Mirica, Isolated Organometallic Nickel(III) and Nickel(IV) Complexes Relevant to Carbon–Carbon Bond Formation Reactions, *J. Am. Chem. Soc.*, 2016, **138**, 12928–12934.

38 W. Zhou, S. Zheng, J. W. Schultz, N. P. Rath and L. M. Mirica, Aromatic Cyanoalkylation through Double C–H Activation Mediated by Ni(III), *J. Am. Chem. Soc.*, 2016, **138**, 5777–5780.

39 S. M. Smith, N. P. Rath and L. M. Mirica, Axial Donor Effects on Oxidatively Induced Ethane Formation from Nickel–Dimethyl Complexes, *Organometallics*, 2019, **38**, 3602–3609.

40 H. Na, M. B. Watson, F. Tang, N. P. Rath and L. M. Mirica, Photoreductive chlorine elimination from a Ni(III)Cl2 complex supported by a tetradentate pyridinophane ligand, *Chem. Commun.*, 2021, **57**, 7264–7267.

41 E. Andris, J. Jašík, L. Gómez, M. Costas and J. Roithová, Spectroscopic Characterization and Reactivity of Triplet and Quintet Iron(IV) Oxo Complexes in the Gas Phase, *Angew. Chem., Int. Ed.*, 2016, **55**, 3637–3641.

42 J. Serrano-Plana, A. Aguinaco, R. Belda, E. García-España, M. G. Basallote, A. Company and M. Costas, Exceedingly Fast Oxygen Atom Transfer to Olefins via a Catalytically Competent Nonheme Iron Species, *Angew. Chem., Int. Ed.*, 2016, **55**, 6310–6314.

43 J. Serrano-Plana, W. N. Oloo, L. Acosta-Rueda, K. K. Meier, B. Verdejo, E. García-España, M. G. Basallote, E. Münck, L. Que, A. Company and M. Costas, Trapping a Highly Reactive Nonheme Iron Intermediate That Oxygenates Strong C—H Bonds with Stereoretention, *J. Am. Chem. Soc.*, 2015, **137**, 15833–15842.

44 V. Dantignana, J. Serrano-Plana, A. Draksharapu, C. Magallón, S. Banerjee, R. Fan, I. Gamba, Y. Guo, L. Que, M. Costas and A. Company, Spectroscopic and Reactivity Comparisons between Nonheme Oxoiron(IV) and Oxoiron(V) Species Bearing the Same Ancillary Ligand, *J. Am. Chem. Soc.*, 2019, **141**, 15078–15091.

45 C. Magallón, J. Serrano-Plana, S. Roldán-Gómez, X. Ribas, M. Costas and A. Company, Preparation of a coordinatively saturated μ-η2:η2-peroxodicopper(II) compound, *Inorg. Chim. Acta*, 2018, **481**, 166–170.

46 E. Carmona, F. González, M. L. Poveda, J. L. Atwood and R. D. Rogers, Synthesis and properties of dialkyl complexes of nickel(II). The crystal structure of bis(pyridine)bis(trimethylsilylmethyl)nickel(II), *J. Chem. Soc., Dalton Trans.*, 1981, 777–782.

47 E. Carmona, E. Gutierrez-Puebla, J. M. Marin, A. Monge, M. Paneque, M. L. Poveda and C. Ruiz, Synthesis and X-ray structure of the nickelabenzocyclopentene complex [cyclic](Me3P)2Ni(CH2CMe2-o-C6H4). Reactivity toward simple, unsaturated molecules and the crystal and molecular structure of the cyclic carboxylate (Me3P)2Ni(CH2CMe2-o-C6H4C(O)O), *J. Am. Chem. Soc.*, 1989, **111**, 2883–2891.

48 E. Carmona, P. Palma, M. Paneque, M. L. Poveda, E. Gutierrez-Puebla and A. Monge, Synthesis of [cyclic](Me3P)2Ni(CH2CMe2-o-C6H4) and its reactivity toward carbon dioxide, carbon monoxide and formaldehyde. First observation of a carbonyl-carbonate oxidative conproportionation mediated by a transition-metal complex, *J. Am. Chem. Soc.*, 1986, **108**, 6424–6425.

49 N. M. Camasso, A. J. Canty, A. Ariafard and M. S. Sanford, Experimental and Computational Studies of High-Valent Nickel and Palladium Complexes, *Organometallics*, 2017, **36**, 4382–4393.

50 A. J. Canty, A. Ariafard, N. M. Camasso, A. T. Higgs, B. F. Yates and M. S. Sanford, Computational study of C(sp3)–O bond formation at a PdIV centre, *Dalton Trans.*, 2017, **46**, 3742–3748.

51 I. M. Pendleton, M. H. Pérez-Temprano, M. S. Sanford and P. M. Zimmerman, Experimental and Computational Assessment of Reactivity and Mechanism in C(sp3)–N Bond-Forming Reductive Elimination from Palladium(IV), *J. Am. Chem. Soc.*, 2016, **138**, 6049–6060.

52 N. M. Camasso, M. H. Pérez-Temprano and M. S. Sanford, C(sp3)–O Bond-Forming Reductive Elimination from PdIV with Diverse Oxygen Nucleophiles, *J. Am. Chem. Soc.*, 2014, **136**, 12771–12775.

53 M. H. Pérez-Temprano, J. M. Racowski, J. W. Kampf and M. S. Sanford, Competition between sp3-C–N vs sp3-C–F Reductive Elimination from PdIV Complexes, *J. Am. Chem. Soc.*, 2014, **136**, 4097–4100.

54 J. M. Racowski, J. B. Gary and M. S. Sanford, Carbon(sp3)-Fluorine Bond-Forming Reductive Elimination from Palladium(IV) Complexes, *Angew. Chem., Int. Ed.*, 2012, **51**, 3414–3417.

